^{11}C-Loperamide and Its *N-Desmethyl* Radiometabolite Are Avid Substrates for Brain Permeability-Glycoprotein Efflux

Sami S. Zoghbi, Jeih-San Liow, Fumihiko Yasuno, Jinsoo Hong, Edward Tuan, Neva Lazarova, Robert L. Gladding, Victor W. Pike, and Robert B. Innis

Molecular Imaging Branch, National Institute of Mental Health, National Institutes of Health, Bethesda, Maryland

Loperamide, an opiate receptor agonist, does not cross the blood–brain barrier because it is a substrate for the permeability-glycoprotein (P-gp) efflux pump. We evaluated ^{11}C-loperamide as a PET radiotracer to measure P-gp function in vivo. **Methods:** Monkeys were injected with ^{11}C-loperamide, and PET brain images were acquired for 120 min. The baseline scans were followed by scans acquired after administration of either of 2 P-gp inhibitors, (2*R*)-anti-5-{3-[4-(10,11-dichloromethanodibenzo-suber-5-yl)piperazin-1-yl]-2-hydroxypropoxy}quinoline trihydrochloride (DCPQ) or tariquidar. Both the PET scans and ex vivo measurements were obtained in P-gp knockout and wild-type mice. **Results:** Pharmacologic inhibition of P-gp in monkeys dose-dependently increased brain activity, with a 3.7-fold effect at the highest DCPQ dose (8 mg/kg intravenously). This increase of brain activity was not caused peripherally, because DCPQ insignificantly changed the plasma concentration and plasma protein binding of radiotracer. Furthermore, the structurally dissimilar inhibitor, tariquidar, also increased brain uptake with potency equal to that of DCPQ. P-gp knockout mice had 3-fold higher brain activity on PET than did wild-type animals. Four radiometabolites were detected in the plasma and brains of ex vivo mice. The most lipophilic radiometabolite was found to be comobile with reference dLop on high-performance liquid chromatography. The brain concentrations of ^{11}C-loperamide and the putative ^{11}C-dLop were about 16-fold greater in P-gp knockout mice than in wild-type mice. **Conclusion:** Both ^{11}C-loperamide and its putative radiometabolite ^{11}C-dLop are avid P-gp substrates. ^{11}C-dLop may be superior to ^{11}C-loperamide in measuring P-gp function at the blood–brain barrier, because further demethylation of ^{11}C-dLop will generate radiometabolites that have little entry into the brain.

Key Words: ^{11}C-loperamide; P-gp; brain efflux pump; PET; blood–brain barrier

J Nucl Med 2008; 49:649–656
DOI: 10.2967/jnumed.107.047308

The permeability-glycoprotein (P-gp) efflux pump prevents uptake by the brain of drugs from several chemical classes and can transport substances while in the lipid bilayer—namely before they actually cross the membrane (*1*). Substrates for P-gp tend to have both lipophilic components and a positive charge. The lipophilicity causes drugs to be concentrated within the lipid bilayer and thereby exposed to this efflux transporter, which acts as a "hydrophobic vacuum cleaner" (*2*).

A PET radioligand to measure the function of P-gp may be useful, because several human disorders have been associated with abnormal function of this efflux transporter. For example, overexpression of P-gp is partly responsible for multidrug resistance in some cancers, because P-gp blocks the entry of selective chemotherapies into the cytoplasm of the tumor (*1*). Excessive function of P-gp may also be responsible for some cases of resistance to antiepileptic medications, in this case by blocking passage of the medication across the blood–brain barrier (*3*). Finally, decreased function of P-gp at the blood–brain barrier may decrease clearance of amyloid from brain to plasma and thereby predispose individuals to Alzheimer's disease (*4*).

Several substrates of P-gp have been radiolabeled and used in animals or humans to measure P-gp function, including $^{99m/94m}$Tc-sestamibi (*5,6*), ^{11}C-verapamil (*7*), and ^{18}F-paclitaxel (*8*). All these agents have at least one limitation, including difficulty in synthesis (e.g., ^{94m}Tc-sestamibi), significant contamination by radiometabolites (e.g., ^{11}C-verapamil), or low signal-to-noise ratio (i.e., modest increase of brain uptake after P-gp inhibition).

In the search for a better radiotracer for P-gp, we evaluated ^{11}C-loperamide, which has been reported in abstracts to be a promising substrate of this efflux transporter (*9,10*). Loperamide is an opiate agonist that is commonly used to treat diarrhea. It acts on opiate receptors in the gut to slow motility and thereby increase removal of water from stool. Loperamide has low pharmacologic toxicity and is an avid substrate for P-gp at the blood–brain barrier (*11*). For example, despite high doses and high plasma concentrations in human

Received Sep. 13, 2007; revision accepted Dec. 6, 2007.
For correspondence or reprints contact: Sami S. Zoghbi, PhD, National Institute of Mental Health/National Institutes of Health, Molecular Imaging Branch, 31 Center Dr., Room B2-B37, MSC 2035, Bethesda, MD 20892-0135.
E-mail: sami.zoghbi@nih.gov

subjects, loperamide almost completely lacks central nervous system effects, because P-gp efficiently blocks virtually all uptake by the brain. Loperamide is rapidly metabolized in mammals mainly by dealkylation of the dimethyl amide moiety (*12,13*). Some metabolites of loperamide, including *N-desmethyl*-loperamide (*N*-dLop), are predicted to have adequate lipophilicity to enter the brain if not inhibited by P-gp.

We evaluated ^{11}C-loperamide in monkeys and mice as a potential agent for measuring P-gp function, especially with regard to possible contamination of brain activity with radiometabolites. After injection of ^{11}C-loperamide into P-gp knockout mice, we detected the presence of significant amounts of radioactivity with the same chromatographic mobility as the expected major metabolite dLop. We now suggest that this putative radiometabolite, ^{11}C-dLop, may itself have superior properties for measuring P-gp function.

MATERIALS AND METHODS

Materials

GlaxoSmithKline provided *N*-dLop, the precursor for synthesis of ^{11}C-loperamide. Eli Lilly provided (2*R*)-anti-5-{3-[4-(10, 11-dichloromethanodibenzo-suber-5-yl)piperazin-1-yl]-2-hydroxypropoxy}quinoline trihydrochloride (DCPQ), which is a potent inhibitor of P-gp. DCPQ was previously reported as compound **14b** (*14*). Xenova Group, Ltd., provided tariquidar, previously called XR9576 (*15*). Pharmacologic doses in this paper are expressed relative to the trihydrochloride salt of DCPQ and the free base of tariquidar.

In Vitro Receptor Binding

The National Institute of Mental Health Psychoactive Drug Screening Program measured the affinity of loperamide and dLop at 3 opiate receptors (δ, κ, and μ), using radiolabeled agonists for each receptor subtype. Detailed binding protocols are available at http://pdsp.med.unc.edu.

Radiotracer

^{11}C-Loperamide (*10*) was prepared automatically within a lead-shielded hot cell from cyclotron-produced ^{11}C-carbon dioxide in a commercial apparatus (MeI Microlab; Bioscan). ^{11}C-Carbon dioxide (51.8 GBq) was produced according to the ^{14}N(p,α)^{11}C reaction by irradiating nitrogen that contained oxygen (1%) for 20 min at an initial pressure of 11 atmospheres with a proton beam (16.5 MeV; 45 μA) using a PETrace cyclotron (GE Healthcare). The ^{11}C-carbon dioxide was reduced to ^{11}C-methane and further to ^{11}C-iodomethane by repetitive high-temperature direct iodinations (*16*). The ^{11}C-iodomethane was then released from this apparatus in a stream of helium (15 mL/min) into a programmable logic–controlled semirobotic Synthia apparatus (Synthia; Uppsala University PET Centre). The helium containing ^{11}C-iodomethane was bubbled into a septum-sealed 1-mL vial containing a solution of *N*-dLop (1.5 mg, 3.25 μmol) and potassium hydroxide (5.0 mg, 89.3 μmol) in 400 μL of anhydrous dimethyl sulfoxide. When the radioactivity in the vial maximized, the reaction mixture was heated at 80°C for 6 min and then diluted with water (500 μL). The crude material was injected onto a Luna C_{18} column (10 μm, 10 × 250 mm; Phenomenex) and then eluted at 8 mL/min with 0.1% trifluoroacetic acid:acetonitrile (55:45 v/v). While the eluate was monitored for radioactivity and absorbance at 225 nm (Bioscan HC-003 pin diode for γ-detection; Beckman Gold 166 for ultraviolet absorbance), ^{11}C-loperamide was collected (retention time, 8.7 min) into a 10-mL round-bottom flask and evaporated to dryness. The residue was dissolved in ethyl alcohol (0.5 mL) and 0.9% sodium chloride (10 mL), which was then sterilized by membrane filtration (Millex MP; Millipore) to which sterile sodium bicarbonate for injection (200 μL, 8.4% w/v; Hospira, Inc.) was added aseptically. The pH of the dose was 8.5.

Radiochemical purity was determined on a Prodigy C_{18} column (4.6 × 250 mm, 10 μm; Phenomenex) eluted with 0.1% trifluoroacetic acid:acetonitrile (50:50 v/v) at 2.5 mL/min (retention time, 4.30 min). Identity was confirmed by coinjection with authentic loperamide and observation of its comobility (Beckman Gold 166 for ultraviolet absorbance; Bioscan HC-003 pin diode for γ-detection) and by LC-MS-MS (liquid chromatography/mass spectrometry/mass spectrometry) analysis of associated carrier.

Measurement of *Log $D_{7.4}$*

^{11}C-Loperamide was dissolved in 0.15 M sodium phosphate buffer (pH 7.4) at a specific concentration of about 2.2 MBq/mL. The radiochemical purity of this preparation was greater than 99%. *Log $D_{7.4}$* was determined 6 times at room temperature by extraction of ^{11}C-loperamide into *n*-octanol from the phosphate buffer, as previously described (*17*), but with correction of the radioactivity counts associated with the radiotracer in the aqueous phase after high-performance liquid chromatography (HPLC) analysis.

PET Studies on Nonhuman Primates

Three male rhesus monkeys (*Macaca mulatta;* 11.5 ± 1.4 kg, with these and subsequent data expressed as mean ± SD) were kept fasting overnight, immobilized with ketamine (10 mg/kg intramuscularly), intubated, placed on a ventilator, and anesthetized with 1.6% isoflurane in oxygen. After injecting ^{11}C-loperamide (286 ± 55 MBq intravenously in 4−5 mL; 0.76 ± 0.3 nmol/kg), we acquired dynamic PET scans on either a high-resolution research tomograph (HRRT; Siemens) or the Advance PET tomograph (GE Healthcare), both of which were cross-calibrated. Although these 2 cameras have different resolutions, the regions of interest were large enough to mask this performance difference (*18*). For DCPQ, we obtained a baseline scan in the morning and a P-gp blocked scan in the afternoon for the same animal, with injections separated by 3 h. We administered 3 doses of DCPQ (1, 3, and 8 mg/kg intravenously) and 1 dose of tariquidar (8 mg/kg intravenously), each at 30 min before the radiotracer. For tariquidar, we acquired only a blockade scan and compared it with the baseline scans of 3 other animals.

PET images were coregistered to an MR image template of a monkey brain. Tomographic images were analyzed with PMOD 2.7 (pixelwise modeling computer software; PMOD Group). Regions of interest were drawn on coronal slices. Decay-corrected radioactivity was expressed as percentage standardized uptake value (%SUV), which normalizes for injected activity and body weight.

$$\%\text{SUV} = (\%\,\text{injected activity}/\text{cm}^3\,\text{of brain}) \times (\text{g of body weight}).$$

Plasma Analysis

An intravenous perfusion line, filled with 0.9% sodium chloride, was used for the radiotracer injection. A blood sample (2

mL) was withdrawn before radiotracer administration to determine plasma protein binding, as previously described (*19*). Eight arterial blood samples (0.5 mL each) were drawn into heparin-treated syringes at 15-s intervals until 2 min, followed by 1-mL aliquots at 3, 5, 10, 20, 30, 45, 60, 75, 90, and 120 min. Plasma ^{11}C-loperamide was quantified using radiochromatography (HPLC; methanol:water:triethylamine, 75:25:0.1 by volume at 2.0 mL/min) and γ-counting, as previously described (*19*).

Plasma free fraction was determined at baseline conditions and after administration of DCPQ and tariquidar. Plasma free fraction was measured in triplicate using ultracentrifugation, as described previously (*20*).

PET Studies on Mice

Three knockout mice (28 ± 5 g; *mdr-1a/b*−/−; model 001487-MM, double homozygotes) (*21*) and 3 wild-type mice (31 ± 2 g; *mdr-1a/b*+/+; model FVB) were anesthetized with 1.5% isoflurane and injected via the tail vein with ^{11}C-loperamide, 15.7 ± 2.0 MBq (15.8 ± 2.7 nmol/kg) and 16.8 ± 2.1 MBq (15.7 ± 2.7 nmol/kg), respectively. The injectate ranged in volume from 0.1 to 0.15 mL and was infused over a period of 15–20 s. The mice were purchased from Taconic. One knockout and 1 wild-type mouse were paired and scanned simultaneously on the Advanced Technology Laboratory Animal Scanner (*22*), as previously described (*23*). Serial dynamic images were acquired for 100 min, with frames of 6 × 20 s, 5 × 1 min, 4 × 2 min, 3 × 5 min, 3 × 10 min, and 2 × 20 min. We used a 3-dimensional ordered-subset expectation maximization algorithm to reconstruct data into 17 coronal slices, achieving a resolution of 1.6 mm in full width at half maximum (*24*). The small mouse brain causes little scatter and attenuation of the γ-emissions from ^{11}C; thus, we performed no correction for scatter or attenuation.

Ex Vivo Analysis of Mouse Plasma and Brain

Five P-gp knockout mice (23.5 ± 2.5 g) and 5 wild-type mice (30.2 ± 2.1 g) were anesthetized with 1.5% isoflurane in oxygen, and ^{11}C-loperamide was injected via the tail vein. The knockout mice received 15.2 ± 6 MBq (22.3 ± 7 nmol/kg), and the wild-type mice received 36.4 ± 3 MBq (50.0 ± 20 nmol/kg). At 30 min after radiotracer injection, anticoagulated blood was removed by cardiac puncture, and the brain was harvested. Plasma was separated from whole blood by centrifugation at 1,800*g* for 1 min. Plasma samples were quantified for radioactivity as previously described (*19*) in an automatic γ-counter. Forebrain and cerebellum were separately homogenized using a hand-held tissue Tearor (model 985-370; BioSpec Products Inc.) in a 1.5-times volume of acetonitrile containing carrier loperamide, followed by homogenization with additional H_2O (500 μL). The homogenates were measured in the γ-counter to calculate the percentage recovery of radioactivity into the acetonitrile extracts. The homogenates were then centrifuged at 10,000*g* for 1 min. The clear prefiltered supernatant liquids were injected onto a radio-HPLC Novapak C_{18} column (4 μm, 100 × 8 mm; Waters Corp.) housed in a radial compression module RCM-100 and eluted with methanol:water:triethylamine (75:25:0.1 by volume) at 2.0 mL/min. The eluate was monitored with an in-line flow-through Na(Tl) scintillation detector (Bioscan). Plasma parent and radiometabolite concentrations were calculated as the product of the radio-HPLC fraction of interest and the total plasma radioactivity concentration (dpm/mL). For simultaneous identification and quantification of radioactive dLop and loperamide, internal standards of both nonradioactive compounds were added to the tissue preparations for detection by ultraviolet absorbance.

All animal experiments were performed in accordance with the *Guide for the Care and Use of Laboratory Animals* (*25*) and were approved by the National Institute of Mental Health Animal Care and Use Committee.

RESULTS

Radiotracer

^{11}C-Loperamide was prepared from *N*-dLop with an overall decay-corrected radiochemical yield of 11.3% ± 1.4% and a radiochemical purity of more than 99% (n = 13). The specific activity, decay corrected to the end of synthesis, was 42.6 ± 23.9 GBq/μmol (n = 13), with an average radioactivity of 1.7 ± 0.6 GBq. The overall time of preparation was 37 min. The masses associated with the injected doses were calculated for time of injection.

Measurement of *Log $D_{7.4}$*

The *Log $D_{7.4}$* at room temperature of ^{11}C-loperamide in octanol was 3.04 ± 0.04 (n = 6). The percentage error of the γ-counter measurements of the samples with the least counts was 0.9% ± 0.0% (n = 6). ^{11}C-Loperamide was 99.7% ± 0.1% (n = 4) stable in 0.15 mM sodium phosphate buffer for more than 2 h.

Receptor Screening of Loperamide and *N*-dLop

Loperamide and dLop had high affinity and quite high selectivity for binding to μ-opiate receptors over the δ- and κ-subtypes (Table 1). Loperamide is an agonist; therefore, its affinity was measured using agonist radiotracers.

Metabolism of ^{11}C-Loperamide in Monkeys

At least 6 radiometabolites were detected in monkey arterial plasma. Plasma samples at 15 min showed 2 major radiometabolite peaks (Fig. 1A). The most polar peak (**a**) eluted at the void volume of the column (14.1%), and the other (**e**) immediately before the parent peak (2.6%). The latter peak almost certainly comprises mainly ^{11}C-dLop because of its coelution with authentic dLop under different elution conditions and because this is the expected major metabolite of ^{11}C-loperamide. Three minor peaks (1.7% [**b**], 0.32% [**c**], and 0.24% [**d**]) were detected between the column void volume peak and dLop peaks. These 3 peaks were

TABLE 1
Affinity of Loperamide and dLop for 3 Cloned Human Opiate Receptor Subtypes

Receptor	Agonist radiotracer	K_i (nM)* Loperamide	dLop
μ	^{3}H-DAMGO	0.31 ± 0.03	0.56 ± 0.05
δ	^{3}H-DADLE	116 ± 7	328 ± 22
κ	^{3}H-U69,593	47 ± 4	73 ± 7

*K_i (inhibition constants) values are mean ± SD of 4 competitive binding experiments.

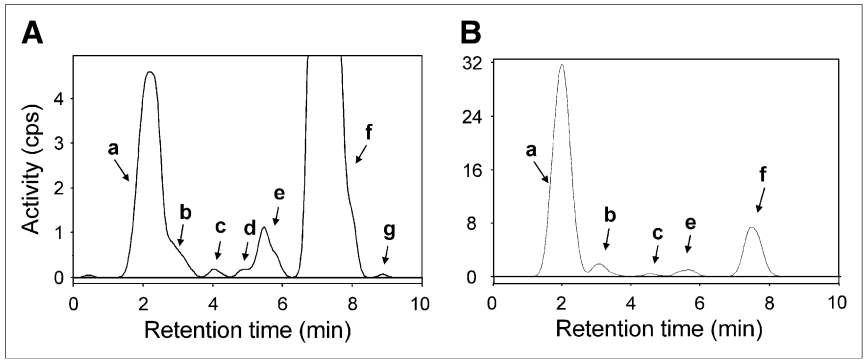

FIGURE 1. Radiochromatogram of activity extracted from plasma of monkey (A) and mouse (B). Monkey plasma was obtained 15 min after intravenous injection of ^{11}C-loperamide, and mouse plasma at 30 min. Radiometabolites **a, b, c, d,** and **e** were more polar than ^{11}C-loperamide peak **f,** but minor peak **g** was more lipophilic than parent.

difficult to resolve at later time points without extending the time of each radiochromatogram and compromising the global information of the arterial input function. Therefore, these 3 radiometabolites were combined and subsequently called radiometabolite B. One minor radiometabolite (0.1%, [**g**]) eluted after the parent peak and was presumably more lipophilic than loperamide.

^{11}C-Loperamide was stable in vitro for 30 min at room temperature in whole blood (93%) and plasma (99%). ^{11}C-Loperamide rapidly metabolized and represented 50% of plasma radioactivity at about 20 min (Fig. 2). The recovery of radioactivity from the standards and all other plasma samples into CH_3CN was 92.5% ± 6.9% (n = 69), with no retention of radioactivity on the HPLC column.

P-gp Inhibition in Monkeys

Preadministration of either of 2 P-gp inhibitors, DCPQ or tariquidar, caused brain activity to increase quickly after injection of ^{11}C-loperamide. Under baseline conditions in 3 monkeys, brain uptake was low (~40% SUV) and quite stable during the 120-min scan (Fig. 3A). Administration of DCPQ 30 min before the radiotracer quickly increased brain activity in a dose-dependent manner. The enhanced brain uptake was apparent within 1–3 min of radiotracer injection and relatively stable thereafter. The lowest dose (1 mg/kg) had minimal effect, but the higher doses (3 and 8 mg/kg) increased brain activity by about 2.5- and 3.5-fold,

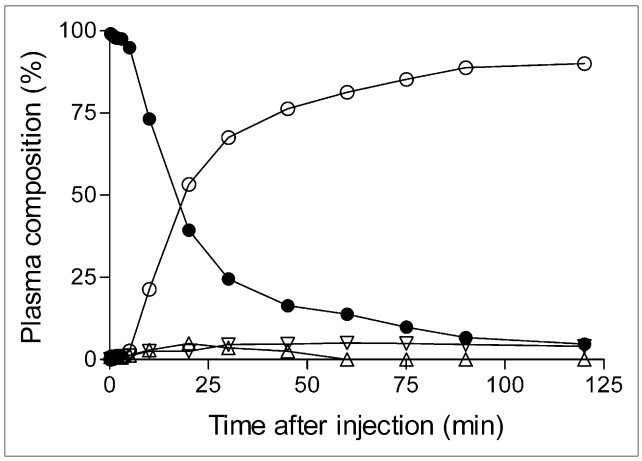

FIGURE 2. Composition of radioactivity extracted from arterial plasma after intravenous injection of ^{11}C-loperamide in monkey. Relative to peaks in Figure 1, loperamide is **f,** dLop is **e,** the most polar is **a,** and pooled intermediates are **b, c,** and **d.** Data are shown for ^{11}C-loperamide (●), dLop (▽), the most polar radiometabolite (○), and the 3 pooled intermediate radiometabolites (△).

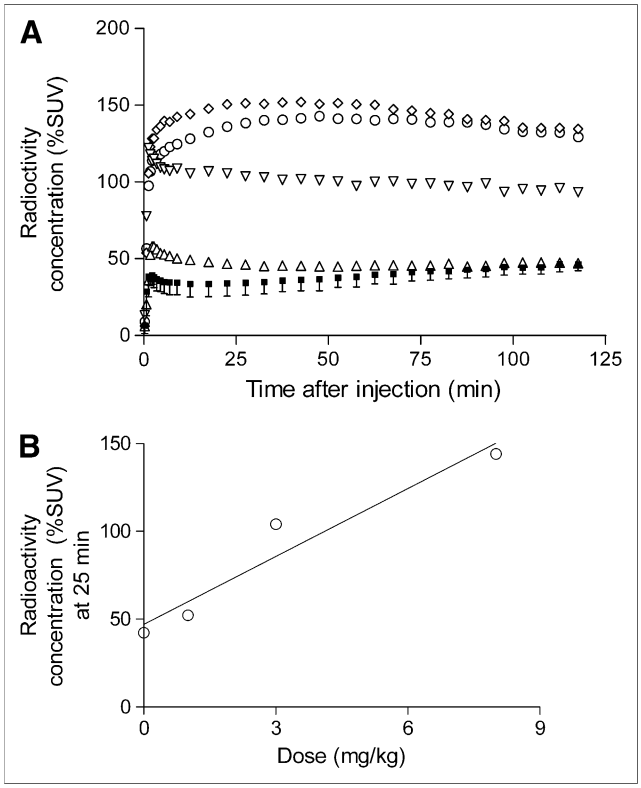

FIGURE 3. Effect of DCPQ and tariquidar on brain uptake of radioactivity in monkey. (A) Brain radioactivity was measured at baseline (■). Unilateral error bars on baseline study are SD from 3 scans. Data are shown for 3 doses of DCPQ (1.0 [△], 3.0 [▽], and 8.0 [◇] mg/kg) and 1 dose of tariquidar (8.0 mg/kg [○]). These P-gp inhibitors were injected intravenously 30 min before ^{11}C-loperamide. Peak radioactivity in brain increased 3.7-fold at dose of 8.0 mg/kg for both tariquidar and DCPQ. Concentrations of radioactivity in brain were corrected for their vascular component, assuming 5% of brain volume. (B) Relationship between DCPQ doses (0, 1, 3, and 8 mg/kg) and concentration of radioactivity (%SUV) at 25 min in monkey forebrain.

respectively (Fig. 3A). Increasing doses of DCPQ caused a linear increase in brain uptake at 25 min and showed no evidence of reaching a maximal effect at 8 mg/kg intravenously (Fig. 3B).

P-gp is widely distributed in the body, including the gastrointestinal tract, liver, and kidneys, and may significantly modulate the metabolism and excretion of drugs. To determine whether the increase in brain activity after DCPQ occurred via a peripheral mechanism, we measured parent radiotracer and radiometabolites in arterial plasma at baseline and after P-gp blockade. At baseline and after DCPQ (8 mg/kg intravenously), the concentration of parent radiotracer quickly decreased and was 50% of total plasma activity at 17 and 20 min, respectively (Fig. 4). The maximal plasma concentration of ^{11}C-loperamide was also similar at baseline (446% SUV) and after DCPQ (408% SUV). As a measure of total exposure to brain, the area under the curve of plasma ^{11}C-loperamide concentration versus time was calculated with a triexponential fit. The area to infinity was 359 at baseline and 417 kBq·min·mL^{-1} after DCPQ. Thus, the almost 3.5-fold increase in forebrain activity could not be explained by a modest 16% increase in plasma exposure. Instead, the effect of DCPQ was likely due to inhibiting P-gp at the blood–brain barrier. To confirm this action, we injected another P-gp inhibitor, tariquidar, whose chemical structure greatly differs from that of DCPQ. Tariquidar was equipotent with DCPQ when both were injected at 8.0 mg/kg intravenously (Fig. 3A).

Finally, increased uptake by the brain after P-gp inhibition was not caused by competitive binding of radiotracer from binding to plasma proteins. DCPQ had a slight but inconsistent effect on the plasma free fraction of ^{11}C-loperamide. At 1.0 mg of DCPQ per kilogram, the plasma free fraction increased 12%, but at doses of 3.0 and 8.0 mg/kg, the plasma free fraction decreased 13% and 8.3%, respectively (Table 2). The plasma free fraction was negligibly affected by tariquidar (8 mg/kg).

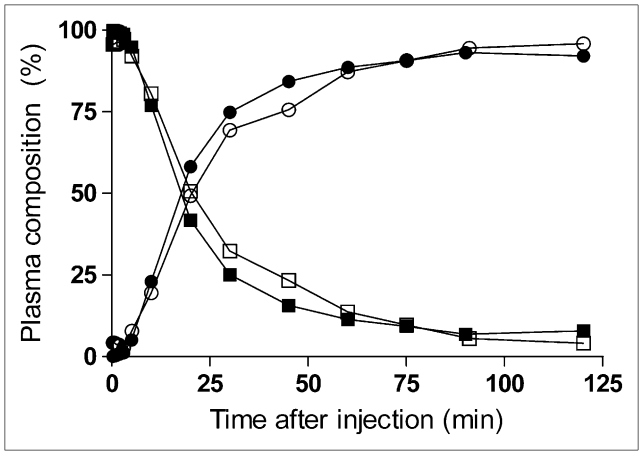

FIGURE 4. Effect of DCPQ on composition of radioactivity in plasma after 2 injections of ^{11}C-loperamide into monkey. Baseline study was performed in morning. DCPQ (8 mg/kg intravenously) was administered 30 min before radiotracer to same monkey in afternoon. All radiometabolites were combined for each study. Data are shown for ^{11}C-loperamide at baseline (□) and after DCPQ (■) and for total radiometabolites at baseline (○) and after DCPQ (●).

PET Studies on Mice

The effect of genetic disruption of P-gp in mice on brain radioactivity uptake after injecting ^{11}C-loperamide was similar to that of pharmacologic inhibition in monkeys. That is, the maximal activity in forebrain and cerebellum of knockout mice was quickly 2.7- and 1.9-fold higher, respectively, than that in wild-type mice (Fig. 5).

At least 4 radiometabolites were detected in plasma, forebrain, and cerebellum of mice after intravenous injection of ^{11}C-loperamide. The radiochromatogram of plasma (Fig. 1B) showed a peak (**a**) that eluted at the void volume of the column. It was the most polar and is designated radiometabolite A in Table 3. The next 3 minor peaks (**b, c,** and **d**) were combined and reported as radiometabolite B. Peak **e** was the most lipophilic radiometabolite and was found to coelute with added authentic dLop. The parent radiotracer (peak **f**) was the most lipophilic and eluted last. Furthermore, peak **e** and reference dLop eluted at a retention time of 5.0 min (10 mL) using a mobile phase of methanol:water: triethylamine, 75:25:0.1 by volume at 2.0 mL/min. The same 2 peaks remained associated after increasing the polarity of the mobile phase (HPLC; methanol:water:triethylamine, 70:30:0.1 by volume at 2.0 mL/min), and the retention time of peak **e** became 7.2 min (14.4 mL). At this extended retention time, peak **e** remained a single and symmetric one. This evidence strongly indicates that this peak is ^{11}C-dLop radiometabolite. Thus, the data are consistent with but do not prove that peak **e** is ^{11}C-dLop.

Uptake of ^{11}C-loperamide and ^{11}C-dLop by the brain was markedly greater in P-gp knockout than in wild-type mice, confirming that both drugs are substrates for this efflux transporter. ^{11}C-Loperamide was increased 16-fold and ^{11}C-dLop 17-fold in forebrain and cerebellum (Table 3). The brain contained other radiometabolites (A and B) that were apparently not substrates and showed minimal differences between animals. These radiometabolites blunted differences between animals such that total radioactivity (i.e.,

TABLE 2
Effect of P-gp Inhibitors on Plasma Free Fraction in Monkey

P-gp inhibitor (mg/kg)	Plasma free fraction		
	Baseline	P-gp inhibition	Percentage difference
DCPQ (1.0)	5.1 ± 0.2	5.7 ± 0.3	+12
DCPQ (3.0)	1.6 ± 0.6	1.4 ± 0.5	−13
DCPQ (8.0)	4.8 ± 1.7	4.4 ± 1.4	−8.3
Tariquidar (8.0)	1.64 ± 0.56	1.71 ± 0.5	+4.3

Values are mean ± SD of at least 3 observations. Percentage difference was calculated relative to baseline.

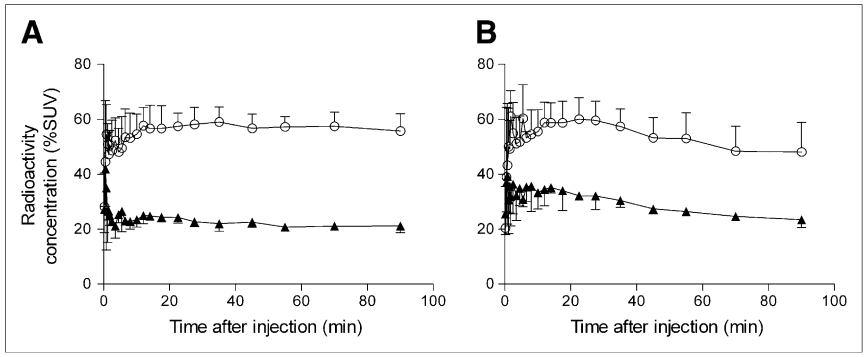

FIGURE 5. PET measurement of radioactivity in forebrain (A) and cerebellum (B) of P-gp knockout (○) and wild-type (▲) mice. Unilateral error bars represent SD for 3 knockout and 3 wild-type mice.

of parent radiotracer and all radiometabolites) in forebrain of P-gp knockout mice was only 4-fold greater than that of wild-type mice (50.9% ± 19.9% SUV vs. 12.5% ± 1.5% SUV, Table 3). These direct ex vivo measurements of total radioactivity are the most relevant to compare with PET, because PET detects radioactivity from all chemical species containing ^{11}C. The direct measurements showed a 4-fold increase in forebrain total radioactivity in knockout animals, compared with wild-type animals (Table 3), whereas PET found only a 2.7-fold increase (Fig. 5).

DISCUSSION

Using the ^{11}C-labeled form, we confirmed that loperamide is an avid substrate for P-gp at the blood–brain barrier in 2 species. Two structurally dissimilar inhibitors, DCPQ and tariquidar, have high affinities to P-gp: 5.3 nM (*26*) and 5.1 nM (*27*), respectively. These inhibitors rapidly increased the brain activity in monkeys. The enhanced uptake was fairly linear in the DCPQ dose range of 1–8 mg/kg intravenously and showed no evidence of a plateau or maximal effect. At the highest dose tested (8 mg/kg intravenously), both DCPQ and tariquidar were equipotent and increased brain activity by about 3.5-fold. We performed comparable studies on mice but used P-gp knockout animals rather than pharmacologic inhibition. PET showed that the brains of knockout mice had about 3-fold greater activity than those of wild-type animals. This enhancement, however, was blunted by the limited anatomic resolution of PET. Ex vivo studies in these mice showed brain activity derived primarily from 2 compounds, the parent radiotracer ^{11}C-loperamide and the radiopeak **e** (Fig. 1), which we deduced to be ^{11}C-dLop metabolite. Unlike PET, these ex vivo measurements were not confounded by limited resolution and its resulting partial-volume errors. The concentrations of ^{11}C-loperamide and ^{11}C-dLop at 30 min were 16- and 17-fold higher in knockout mice than in wild-type mice.

In the light of these results, ^{11}C-dLop may be a better radioprobe than ^{11}C-loperamide for assessing P-gp function at the blood–brain barrier, because the former will have 1 fewer contaminating radiometabolite. The structures of these 2 compounds clarify this point (Fig. 6). When ^{11}C-loperamide is *N*-demethylated, it is anticipated that ^{11}C-methyl and ^{12}C-methyl are equally likely to be removed and subsequently metabolized to $^{11/12}$C-labeled CH_3OH, CH_2O, CO_2H, and CO_2. These compounds in the oxidation route have little entry into the brain (*28*). In contrast to the metabolism of ^{11}C-loperamide, further *N*-demethylation of ^{11}C-dLop leads to radiometabolites, ultimately ^{11}C-CO_2, which has minimal brain entry. Thus, ^{11}C-loperamide is similar to many other P-gp substrate radiotracers by generating radiometabolites that confound PET measurements of brain

TABLE 3
Concentration of ^{11}C-Loperamide and Its Radiometabolites in P-gp Knockout (KO) and Wild-Type (WT) Mice

	Forebrain			Cerebellum			Plasma		
	Concentration (%SUV)*			Concentration (%SUV)*			Concentration (%SUV)*		
Radiochemical species	KO	WT	KO/WT ratio	KO	WT	KO/WT ratio	KO	WT	KO/WT ratio
Radiometabolite A	10.9 ± 2.7	10.2 ± 2.0	1	11.2 ± 5.7	10.3 ± 2.2	1	19.3 ± 5.6	20.5 ± 3.6	0.9
Radiometabolite B§	2.6 ± 2.1	0.3 ± 0.1	9	2.4 ± 1.6	0.3 ± 0.1	8	1.9 ± 0.4	2.1 ± 1.0	0.9
^{11}C-dLop	12.1 ± 6.4	0.7 ± 0.2	17	14.4 ± 5.9	1.1 ± 0.5	13	0.8 ± 0.3	0.9 ± 0.1	0.9
^{11}C-Loperamide	25.4 ± 10.6	1.6 ± 0.4	16	16.9 ± 7.8	1.5 ± 1.0	11	6.3 ± 3.3	7.8 ± 1.3	0.8
Total radioactivity	50.9 ± 19.9	12.5 ± 1.5	4	44.9 ± 16.5	13.4 ± 0.9	3	28.3 ± 7.5	31.2 ± 1.1	0.9

*Data are mean ± SD.
§Values are sum total of radiometabolites **b, c,** and **d** (Fig. 1).
Five P-gp knockout and 5 wild-type mice were killed 30 min after intravenous injection of ^{11}C-loperamide.

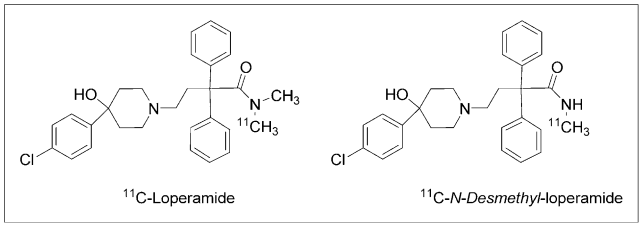

FIGURE 6. Chemical structures of ^{11}C-loperamide and ^{11}C-dLop.

activity. In this case, however, the confounding metabolite, ^{11}C-dLop, may itself be a superior PET radiotracer.

Inactivation of P-gp function with either pharmacologic inhibition in monkeys or genetic knockout in mice caused a rapid and sustained increase of brain activity after injection of ^{11}C-loperamide. The enhanced uptake was near maximal within a few minutes after injection in both monkeys and mice. The rapid effect of P-gp inhibition is consistent with this efflux pump's blocking entry rather than facilitating removal of radiotracer. Although both would have the same net effect, facilitating removal would likely be a slower process, first allowing entry, then diffusion in extracellular space, and finally removal from brain. In fact, the current model for P-gp function proposes that drugs are removed while in the membrane lipid bilayer (*1*)—that is, before they enter the extracellular space of the brain.

Compared with ex vivo measurements, PET brain imaging was confounded by limited anatomic resolution and contamination from radiometabolites. The more accurate ex vivo measurements demonstrated markedly increased concentrations of ^{11}C-loperamide (16-fold) and ^{11}C-dLop (17-fold) in P-gp knockout brain, compared with wild-type brain. These high ratios reflect, in part, the thoroughness of P-gp in blocking entry of these 2 compounds to the brain. That is, the denominator of the ratio (brain uptake in wild-type mice) is extraordinarily low, thus having significant implications for PET. Although one can measure decreased P-gp function as increased tissue radioactivity, one would likely not be able to measure enhanced P-gp function, because tissue radioactivity is already at almost immeasurably low levels. For example, some cases of drug resistance in epilepsy may be caused by locally enhanced P-gp function—and thus drug removal—at the epileptogenic focus (*3*). ^{11}C-Loperamide and ^{11}C-dLop would likely be unable to measure such increased P-gp function, because baseline activity is so low, at least in nonhuman primates. In this regard, a less avid P-gp substrate radiotracer would be superior to loperamide for measuring enhanced P-gp function.

Did ^{11}C-loperamide and ^{11}C-dLop show measurable binding to opiate receptors in vivo? μ-Opiate receptors have significantly higher densities in the forebrain than in the cerebellum of mice (*29*). Thus, if the radiotracer has significant receptor binding greater than nonspecific levels, its concentration should be higher in forebrain than in cerebellum. Our PET data are not useful for addressing this question, because partial-volume errors will cross-contaminate the cerebellum and forebrain and because the PET measurements of total radioactivity are contaminated by several radiometabolites. In contrast, the ex vivo data have no partial-volume errors and can separately identify ^{11}C-loperamide and ^{11}C-dLop by radiochromatography. At 30 min after injection in knockout mice, the ratio of concentration in the forebrain to concentration in the cerebellum was 1.5 for ^{11}C-loperamide (25.4% vs. 16.9%) and about 1 for ^{11}C-dLop (12.1% vs. 14.4%). One-way ANOVA demonstrated that there was no significant brain regional differences ($\alpha = 0.05$) in the distribution of either radiochemical species. Although we have no evidence of specific in vivo binding of the radiotracer to μ-opiate receptors, this issue deserves additional study in the future.

CONCLUSION

^{11}C-Loperamide and its putative *N-desmethyl* metabolite, ^{11}C-dLop, are avid substrates for P-gp efflux at the blood–brain barrier. ^{11}C-dLop may have properties superior to those of the parent radiotracer for measuring P-gp function, because further demethylation of the former generates radiometabolites that have limited entry into the brain.

ACKNOWLEDGMENTS

The Intramural Research Program of NIMH supported this research (project Z01-MH-002795-04). We thank GlaxoSmithKline for providing *N*-dLop, the staff of the NIH PET Department for successfully performing the monkey PET studies, PMOD Technologies for providing its image analysis software, and the NIMH Psychoactive Drug Research Program for measuring the in vitro affinity of loperamide and dLop at opiate receptors subtypes.

REFERENCES

1. Gottesman MM, Fojo T, Bates SE. Multidrug resistance in cancer: role of ATP-dependent transporters. *Nat Rev Cancer.* 2002;2:48–58.
2. Raviv Y, Pollard HB, Bruggemann EP, Pastan I, Gottesman MM. Photosensitized labeling of a functional multidrug transporter in living drug-resistant tumor cells. *J Biol Chem.* 1990;265:3975–3980.
3. Siddiqui A, Kerb R, Weale ME, et al. Association of multidrug resistance in epilepsy with a polymorphism in the drug-transporter gene ABCB1. *N Engl J Med.* 2003;348:1442–1448.
4. Vogelgesang S, Cascorbi I, Schroeder E, et al. Deposition of Alzheimer's beta-amyloid is inversely correlated with P-glycoprotein expression in the brains of elderly non-demented humans. *Pharmacogenetics.* 2002;12:535–541.
5. Piwnica-Worms D, Chiu M, Budding M, Kronauge J, Kramer R, Croop J. Functional imaging of multidrug-resistant P-glycoprotein with an organotechnetium complex. *Cancer Res.* 1993;53:977–984.
6. Bigott HM, Prior J, Piwnica-Worms D, Welch M. Imaging multidrug resistance P-glycoprotein transport function using microPET with technetium-94m-sestamibi. *Mol Imaging.* 2005;4:30–39.
7. Takano A, Kusuhara H, Suhara T, et al. Evaluation of in vivo P-glycoprotein function at the blood–brain barrier among MDR1 gene polymorphisms by using ^{11}C-verapamil. *J Nucl Med.* 2006;47:1427–1433.
8. Kurdziel KA, Kiesewetter D, Carson R, Eckelman W, Herscovitch P. Biodistribution, radiation dose estimates, and in vivo Pgp modulation studies of ^{18}F-paclitaxel in nonhuman primates. *J Nucl Med.* 2003;44:1330–1339.
9. Passchier J, Lawrie K, Bender D, Fellows I, Gee A. [^{11}C]Loperamide as highly sensitive PET probe for measuring changes in P-glycoprotein functionality [abstract]. *J Labelled Comp Radiopharm.* 2003;46(suppl):S403.

10. Wilson A, Passchier J, Garcia A, et al. Production of the P-glycoprotein marker, [^{11}C]loperamide, in clinically useful quantities [abstract]. *J Labelled Comp Radiopharm.* 2005;48(suppl):S142.
11. Choo EF, Kurnik D, Muszkat M, et al. Differential in vivo sensitivity to inhibition of P-glycoprotein located in lymphocytes, testes, and the blood-brain barrier. *J Pharmacol Exp Ther.* 2006;317:1012–1018.
12. Kalgutkar AS, Nguyen H. Identification of an N-methyl-4-phenylpyridinium-like metabolite of the antidiarrheal agent loperamide in human liver microsomes: underlying reason(s) for the lack of neurotoxicity despite the bioactivation event. *Drug Metab Dispos.* 2004;32:943–952.
13. Yoshida K, Nambu K, Arakawa S, Miyazaki H, Hashimoto M. Metabolites of loperamide in rats. *Biomed Mass Spectrom.* 1979;6:253–259.
14. Pfister JR, Makra F, Muehldorf AV, et al. Methanodibenzosuberylpiperazines as potent multidrug resistance reversal agents. *Bioorg Med Chem Lett.* 1995;5: 2473–2476.
15. Roe M, Folkes A, Ashworth P, et al. Reversal of P-glycoprotein mediated multidrug resistance by novel anthranilamide derivatives. *Bioorg Med Chem Lett.* 1999;9:595–600.
16. Larsen P, Ulin J, Dahlstrøm K, Jensen M. Synthesis of [^{11}C]iodomethane by iodination of [^{11}C]methane. *Appl Radiat Isot.* 1997;48:153–157.
17. Zoghbi SS, Baldwin RM, Seibyl JP, Charney DS, Innis RB. A radiotracer technique for determining apparent pK_a of receptor-binding ligands. *J Labelled Comp Radiopharm.* 1997;40SI:136–138.
18. Imaizumi M, Briard E, Zoghbi SS, et al. Kinetic evaluation in nonhuman primates of two new PET ligands for peripheral benzodiazepine receptors in brain. *Synapse.* 2007;61:595–605.
19. Zoghbi SS, Shetty UH, Ichise M, et al. PET imaging of the dopamine transporter with ^{18}F-FECNT: a polar radiometabolite confounds brain radioligand measurements. *J Nucl Med.* 2006;47:520–527.
20. Gandelman MS, Baldwin RM, Zoghbi SS, Zea-Ponce Y, Innis RB. Evaluation of ultrafiltration for the free fraction determination of SPECT radiotracers: β-CIT, IBF, and iomazenil. *J Pharm Sci.* 1994;83:1014–1019.
21. Schinkel AH, Wagenaar E, Mol C, van Deemter L. P-glycoprotein in the blood-brain barrier of mice influences the brain penetration and pharmacological activity of many drugs. *J Clin Invest.* 1996;97:2517–2524.
22. Seidel J, Vaquero JJ, Green MV. Resolution uniformity and sensitivity of the NIH ATLAS small animal PET scanner: comparison to simulated LSO scanners without depth-of-interaction capability. *IEEE Trans Nucl Sci.* 2003;50:1347–1350.
23. Liow JS, Lu S, McCarron JA, et al. Effect of a P-glycoprotein inhibitor, cyclosporin A, on the disposition in rodent brain and blood of the 5-HT_{1A} receptor radioligand, [^{11}C](*R*)-(−)-RWAY. *Synapse.* 2007;61:96–105.
24. Johnson CA, Seidel J, Vaquero JJ, Pascau J, Desco M, Green MV. Exact positioning for OSEM reconstructions on the ATLAS depth-of-interaction small animal scanner [abstract]. *Mol Imaging Biol.* 2002;4(suppl):S22.
25. Clark J, Baldwin R, Bayne K, et al. *Guide for the Care and Use of Laboratory Animals.* Washington, DC: Institute of Laboratory Animal Resources, National Research Council; 1996.
26. Ekins S, Kim RB, Leake BF, et al. Application of three-dimensional quantitative structure-activity relationships of P-glycoprotein inhibitors and substrates. *Mol Pharmacol.* 2002;61:974–981.
27. Martin C, Berridge G, Mistry P, Higgins C, Charlton P, Callaghan R. The molecular interaction of the high affinity reversal agent XR9576 with P-glycoprotein. *Br J Pharmacol.* 1999;128:403–411.
28. Gunn RN, Ranicar A, Yap JT, et al. On-line measurement of exhaled [^{11}C]CO_2 during PET. *J Nucl Med.* 2000;41:605–611.
29. Pert CB, Kuhar MJ, Snyder SH. Opiate receptor: autoradiographic localization in rat brain. *Proc Natl Acad Sci USA.* 1976;73:3729–3733.